Proc. Natl. Acad. Sci. USA
Vol. 93, pp. 10729–10734, October 1996
Biochemistry

DNA strand annealing is promoted by the yeast Rad52 protein

(genetic recombination/repair/*Saccharomyces cerevisiae*)

UFFE H. MORTENSEN†, CHRISTIAN BENDIXEN‡, IVANA SUNJEVARIC§, AND RODNEY ROTHSTEIN¶

Department of Genetics and Development, College of Physicians and Surgeons, Columbia University, 701 West 168th Street, New York, NY 10032

Communicated by Paul Berg, Stanford University Medical Center, Stanford, CA, July 3, 1996 (received for review May 8, 1996)

ABSTRACT **The *Saccharomyces cerevisiae RAD52* gene plays a pivotal role in genetic recombination. Here we demonstrate that yeast Rad52 is a DNA binding protein. To show that the interaction between Rad52 and DNA is direct and not mediated by other yeast proteins and to facilitate protein purification, a recombinant expression system was developed. The recombinant protein can bind both single- and double-stranded DNA and the addition of either Mg^{2+} or ATP does not enhance the binding of single-stranded DNA. Furthermore, a DNA binding domain was found in the evolutionary conserved N terminus of the protein. More importantly, we show that the protein stimulates DNA annealing even in the presence of a large excess of nonhomologous DNA. Rad52-promoted annealing follows second-order kinetics and the rate is 3500-fold faster than that of the spontaneous reaction. How this annealing activity relates to the genetic phenotype associated with *rad52* mutant cells is discussed.**

An important aspect of DNA metabolism is homology dependent recombination and double-strand break repair. *RAD52* is the defining member of an epistasis group involved in these complex processes. Among these genes are *RAD54*, a putative ATPase in the *SNF/SWI* family (1, 2), and the RecA homologs: *RAD51*, *RAD55*, *RAD57*, and *DMC1* (3–6). So far, only the Rad51 gene product has been characterized biochemically in detail. Like RecA, it forms a filament on DNA and catalyzes strand exchange in the presence of ATP (7–9). Notably, the polarity of the Rad51-catalyzed strand-transfer reaction is opposite to that of RecA (9). These results, combined with the fact that several different RecA homologs exist, imply that not all recombination processes in yeast are completely analogous to those found in *Escherichia coli*. In addition, there are genes in yeast that have unknown but important roles in recombination. In this study, we focus on the function of Rad52 in these processes.

Originally, yeast cells containing *rad52* mutations were identified by their extreme sensitivity to X-irradiation (10). Genetic studies subsequently established the central role of *RAD52* in genetic recombination and double-strand break repair (11–13). For example, *rad52* mutants are severely impaired in their commitment to meiotic recombination and essentially no viable spores are produced (14–16). Furthermore, in most cases, mitotic recombination also requires a functional *RAD52* gene (15, 17, 18). The importance of the yeast *RAD52* gene is underscored by the presence of homologs in all eukaryotic organisms investigated to date (19–22).

The *RAD52* gene was cloned and sequenced more than 12 years ago (23, 24); however, no indication of its biochemical function has been revealed from the primary structure. Although Rad52 has been reported to possess a weak strand transfer activity (25), thus far only an interaction with Rad51 has been firmly established biochemically (26, 27). Recently, genetic experiments suggested that Rad52 interacts with RP-A through the largest subunit of this single-stranded (ss) DNA binding protein (28). Preliminary results showed a physical interaction that is dependent on the presence of DNA (U.H.M., J. Smith, and R.R., unpublished results). Therefore, we examined the possibility that Rad52 protein interacts directly with DNA and we found that it dramatically stimulates DNA annealing.

MATERIALS AND METHODS

Yeast Strains, Extract Preparation, and Protein Blotting. *RAD52 pep4* and *rad52-8::TRP1 pep4* yeast strains were isogenic to W303 (29). Cells were harvested from a 5-ml culture grown to mid-log phase. Extracts were prepared by lysing the cells using glass beads in 50 mM Tris (pH 8.0), 500 mM NaCl, 1% Nonidet P-40 in the presence of protease inhibitors [0.1 mM phenylmethylsulfonyl fluoride (PMSF)/10 mM benzamidine/100 μg/ml bacitracin/1 μg/ml pepstatin A]. Extracts were diluted 5-fold in 50 mM Tris (pH 8.0), including protease inhibitors to a total volume of 2.5 ml and applied to 0.5 ml of ssDNA cellulose (Pharmacia). The columns were eluted by 1-ml steps of 0.2, 0.3, 0.4, 0.5, 0.6, or 1.0 M NaCl in 20 mM Tris (pH 8.0). Anti-Rad52 serum was obtained by injecting several rabbits at a commercial facility (Pocono Rabbit Farm, Canadensis, PA) with a fragment of Rad52 (aa 93–315) fused to glutathione *S*-transferase. Anti-Rad52 serum was used without further purification. Proteins were separated by SDS/PAGE (12% homogeneous gel) and transferred to an Immobilon-P membrane (Millipore). Next, the membrane was probed with a 1000-fold dilution of the anti-Rad52 serum and the resulting immunocomplexes visualized using an enhanced chemiluminescence kit (Amersham).

Expression and Purification of Recombinant Rad52 Protein. There are six putative start codons near the N terminus of the *RAD52* gene and the position of the *in vivo* start codon is unknown. Because the other homologs of *RAD52* contain no identity with the first 34 amino acids (19–22) and an attempt to express Rad52 from the first start codon was unsuccessful, recombinant Rad52 protein (hereafter referred to as Rad52*) used in this study was generated from the third start codon. Expression from the third start codon of *RAD52* has been shown to be functionally competent (30). A PCR-generated fragment of *RAD52* encoding aa 34–504 was ligated into the *Nco*I site of pQE60 (Qiagen, Chatsworth, CA) thus, fusing the C terminus of this open reading frame with a His_6 tag (pQE60-Rad52*-His_6). The His_6 tag allows simple purification using an Ni–NTA agarose (Qiagen). We have shown that a His_6 tag in the C terminus of Rad52 does not interfere with its capacity to repair double-strand breaks and to integrate a

The publication costs of this article were defrayed in part by page charge payment. This article must therefore be hereby marked "*advertisement*" in accordance with 18 U.S.C. §1734 solely to indicate this fact.

Abbreviations: ss, single stranded; ds, double stranded.

†Present address: Department of Chemistry, Carlsberg Laboratory, Valby DK-2500 Copenhagen, Denmark.
‡Present address: Danish Institute of Animal Science, Research Centre Foulum, P.O. Box 39, DK-8830 Tjele, Denmark.
§On leave of absence from: Institute Boris Kidrich, Vinca, Yugoslavia.
¶To whom reprint requests should be addressed. e-mail: rothstein@cuccfa.ccc.columbia.edu.

homologous DNA fragment into a chromosomal target (unpublished results). The pQE60-Rad52-169*-His_6 plasmid contains a fragment of *RAD52* encoding aa 34–169 in-frame with the His_6 tag and was constructed from pQE60-Rad52*-His_6 by fusing the *Bgl*II site within the Rad52 open reading frame with the *Bam*HI in the plasmid backbone. Plasmids were introduced into *E. coli* strain M15(pREP4) and induced by growing a 1 liter culture in Luria broth, OD_{600} = 1, for 30 min in the presence of 1 mM isopropyl β-D-thiogalactoside at 37°C. Cells were lysed on ice by sonication using a Sonicator W-385 (Heat Systems–Ultrasonics, Farmingdale, NY) in 15 ml of 50 mM NaH_2PO_4 (pH 8.0), 300 mM NaCl in the presence of 10 mg/ml lysozyme and protease inhibitors (0.1 mM PMSF/10 mM benzamidine/100 μg/ml bacitracin/1 μg/ml pepstatin A). After lysis, polymin P (Sigma) was added to a final concentration of 0.08% vol/vol and cell debris was spun down by centrifugation for 10 min at 12,000 rpm at 4°C. The supernatant was applied to 20 ml of Ni–NTA agarose (Qiagen) and the resin washed with 20 vol of 50 mM Tris (pH 6), 300 mM NaCl, 100 mM imidazole, 10% glycerol. Rad52* and Rad52-169* were eluted with 50 mM Tris, 300 mM NaCl, 500 mM imidazole (pH 6), 10% glycerol. Fractions of the Rad52* eluate or Rad52-169* eluate from Ni–NTA columns were diluted by adding 3 vol of 20 mM Tris (pH 8.0)/10% glycerol, applied to 1.0 ml of ssDNA cellulose and the flow-through collected. The columns were washed with 5 vol of a buffer composed of 1 vol of 50 mM Tris, 300 mM NaCl, 500 mM imidazole (pH 6), and 3 vol of 20 mM Tris (pH 8.0)/10% glycerol (i.e., the same composition as the applied sample), and then with 10 vol of 20 mM Tris (pH 8), 0.1 M NaCl, 10% glycerol. The columns were eluted with 5-ml steps of 0.2, 0.3, 0.4, 0.5, 0.6, and 1.0 M NaCl in 20 mM Tris (pH 8.0)/10% glycerol or 0.2 and 1.0 M NaCl in 20 mM Tris (pH 8.0)/10% glycerol in the case of Rad52* or Rad52-169*, respectively. Aliquots from the indicated steps in the elution profiles were separated using SDS/12% PAGE and visualized by Coomassie brilliant blue G-250 (Bio-Rad).

DNA Binding Assays. Rad52* and BSA were coupled to CNBr-activated Sepharose 4B (Pharmacia) according to the manufacturer's instructions. The coupling efficiency was close to 90% in both cases, as determined by the difference in OD_{280} of the solution before and after the coupling reaction. The resins were equilibrated in 20 mM Tris (pH 8.3) at 4°C before use. Analysis of DNA binding was performed at 4°C. ssDNA and double-stranded (ds) DNA were represented by defined oligonucleotides (oligo-A: 5′-CTTCGTTATCGTTTCGTCAGGATCACTCACCAGAGGAAGCTCCGGAAGCTCCG-3′ and oligo-B: 5′-CGGAGCTTCCGGAGCTTCCTCTGGTGAGTGATCCTGACGAAACGATAACGAAG-3′). Oligo-A was ^{32}P end-labeled and used as the ssDNA. dsDNA was made by boiling 40 μl of a 25 nM ^{32}P end-labeled oligo-A and 50 nM oligo-B mixture and, subsequently, allowing it to cool slowly at room temperature. The DNA samples were diluted into 20 mM Tris (pH 8.3) and applied to 0.75 ml Rad52*-Sepharose. The column was eluted with 1.5-ml steps of 0.2, 0.3, 0.4, 0.5, 0.6, or 1.0 M NaCl in 20 mM Tris (pH 8.0). The effect of 10 mM Mg^{2+} and 2 mM ATP was evaluated in combination and individually. The samples were analyzed by 15% PAGE (Bio-Rad) and the presence of DNA was visualized by a PhosphorImager 445 SI/IMAGEQUANT (Molecular Dynamics).

DNA Annealing Reactions. Annealing reactions were carried out in 50 μl of 20 mM Tris (pH 8.0)/100 mM NaCl at 25°C for 1 hr. The reactions were terminated by the addition of SDS, proteinase K, and unlabeled oligo-D at a final concentration of 0.4%, 0.77 mg/ml and 1.54 μM, respectively, and incubated for 5 min at room temperature. The concentration of Rad52* was determined using a modified Lowry assay (Bio-Rad). In Fig. 4*C*, 500-μl reactions were started and 50-μl aliquots were taken at various times (1, 3, 5, 10, 15, 20, 30, and 60 min). The 0 time point was obtained by adding the stop mixture to an aliquot of the protein solution before adding DNA. In Fig. 4*D*, annealing was performed with equimolar concentrations of oligo-C and oligo-D. Equimolar concentrations of the oligonucleotides were obtained by annealing 200 pmol of ^{32}P end-labeled oligo-D with 800 pmol of oligo-C in a total volume of 40 μl. This mixture was boiled and subsequently allowed to cool slowly to room temperature. The resulting Y-structure was separated from excess single-stranded oligonucleotides on a 15% polyacrylamide gel. The band containing the Y-structure was isolated and the DNA recovered from the gel slice by eluting it in 500 μl of water for 24 hr at room temperature. The DNA was concentrated by butanol extraction followed by ethanol precipitation. The pellet was resuspended in 100 μl of 100 mM NaCl/20 mM Tris (pH 8.0). Before each annealing reaction, the DNA-containing sample was incubated at 95°C for 5 min and then quickly transferred to an ice/water slurry. All annealing reactions were performed in a volume of 40 μl of 100 mM NaCl/20 mM Tris (pH 8.0) at 25°C. Rad52*-stimulated annealing reactions were initiated by mixing 20 μl of DNA with 20 μl of 180 nM Rad52*, both present in 100 mM NaCl/20 mM Tris (pH 8.0) and preheated for 5 min at 25°C before being mixed. Aliquots (3 μl) were withdrawn from the annealing reactions at various time points and diluted into 97 μl (spontaneous reaction) or 27 μl (the Rad52*-stimulated reaction) of 0.5% SDS/1 mg/ml proteinase K incubated at room temperature for 5 min and stored on ice. The half-time of each reaction was based on nine individual time points. Samples were analyzed by 15% PAGE and the amount of DNA was visualized and quantified using a PhosphorImager 445 SI/IMAGEQUANT (Molecular Dynamics).

RESULTS

Rad52 Is a DNA Binding Protein. A yeast extract was applied to an ssDNA cellulose column and the bound material was eluted with salt. The different fractions were probed in a Western blot using a Rad52 antibody (Fig. 1*A*). Because several proteins in the extract were recognized by the antibody, we analyzed a similar extract from a strain containing a disruption of the *RAD52* gene (Fig. 1*B*). By comparing the band patterns obtained from each extract, we identified one band that was present only in the wild-type extract (arrow). More importantly, this band represents the only protein eluting from the ssDNA cellulose column that can be detected with the Rad52 antibody (Fig. 1*A*).

Next, we examined whether purified recombinant Rad52* protein from *E. coli* also binds to an ssDNA cellulose resin. The elution profile showed that no protein was visible in the flow-through and that bound Rad52* eluted at similar salt concentrations as Rad52 present in yeast extracts (Fig. 2*A*). Thus, recombinant Rad52* behaved similarly to native Rad52,

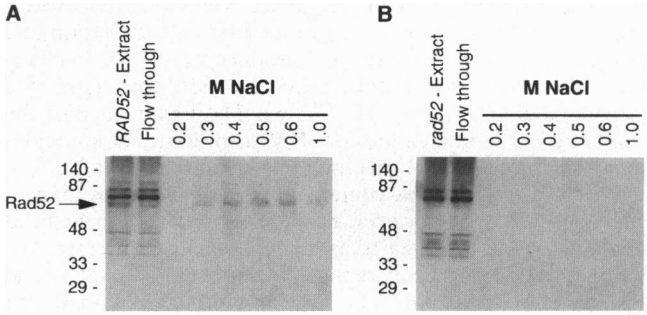

FIG. 1. Rad52 from yeast binds ssDNA. Fractionation of extracts on ssDNA cellulose using W303 derivatives (29) is shown. (*A*) *RAD52 pep4* and (*B*) *rad52-8::TRP1 pep4*. Aliquots from the indicated steps in the elution profile were separated using SDS/12% PAGE, transferred to an Immobilon-P membrane (Millipore), and probed with anti-Rad52 serum.

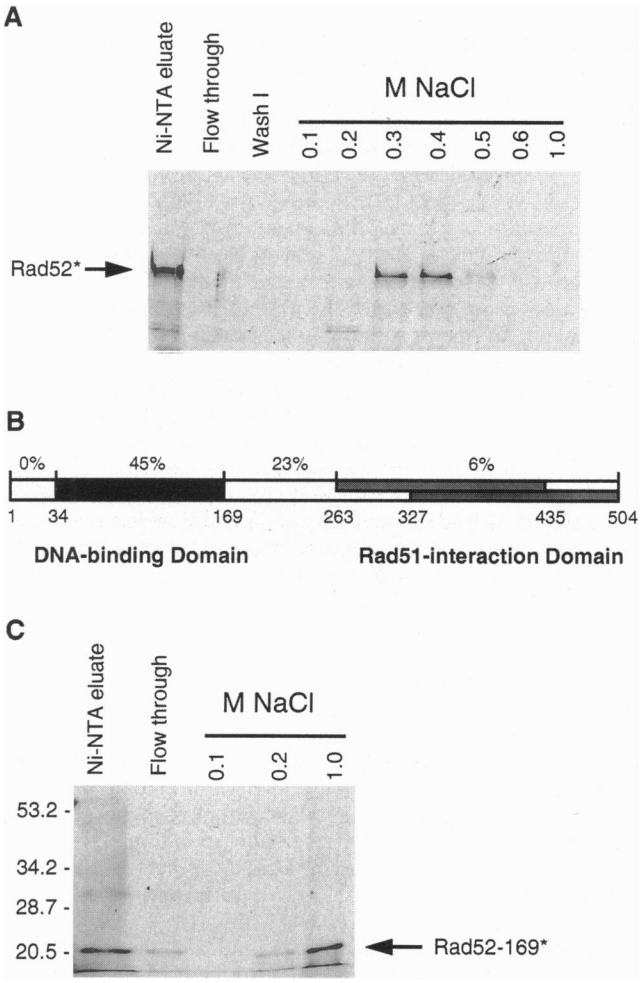

FIG. 2. Recombinant Rad52* protein binds ssDNA. (*A*) Rad52* binds to ssDNA cellulose. A diluted fraction of the Rad52* eluate from an Ni–NTA column was applied to ssDNA cellulose and the flow-through collected. The column was washed and then eluted by increasing the salt concentration. Aliquots from the indicated steps in the purification profile were separated using SDS/12% PAGE and visualized by Coomassie brilliant blue G-250. (*B*) A map of the functional domains of Rad52. The yeast Rad52 protein was compared with the mouse sequence using our previously published alignment (22). The percentage identity within domains is shown. The extent of the Rad51p-interacting domains shown is based on our results (unpublished results) (upper bar) and those of Milne and Weaver (26) (lower bar). (*C*) The N-terminal fragment, Rad52-169*, binds to ssDNA cellulose. A diluted fraction of the Rad52-169* eluate from an Ni–NTA column was applied to ssDNA cellulose and the flow-through collected. The column was washed and then eluted by increasing the salt concentration. Samples from the indicated steps in the purification profile were separated using SDS/12% PAGE and visualized by Coomassie brilliant blue G-250.

showing that the interaction between the protein and DNA is direct and not mediated by additional proteins present in the yeast extract. Furthermore, DNA binding was found to be an evolutionarily conserved feature of Rad52, because mouse Rad52 obtained by *in vitro* translation binds ssDNA cellulose in a similar manner (unpublished results).

Because the N terminus of Rad52 is the most conserved region when the primary structures from different species are compared (Fig. 2*B*), we tested whether a 136-aa N-terminal fragment (see *Materials and Methods*) could mediate the DNA interaction. A protein in the expected size range was eluted from the Ni–NTA column and this protein fragment bound to and eluted from the ssDNA cellulose column in a manner similar to Rad52*. The N-terminal location of a DNA binding domain is reasonable because the C-terminal end mediates the physical interaction to Rad51. The finding that Rad52* binds ssDNA cellulose was used to purify further the Rad52* protein obtained from the Ni–NTA column.

Initially, the substrate specificity of Rad52* was investigated by testing ssDNA and dsDNA oligonucleotides for their affinity to Rad52*-Sepharose. Both forms of DNA were retained on Rad52*-Sepharose, but the ssDNA oligonucleotide eluted at a slightly higher salt concentration than the dsDNA oligonucleotide indicating a slight preference for ssDNA (Fig. 3). The coupling of Rad52* to Sepharose did not affect its ability to bind DNA, since the ssDNA oligonucleotide eluted from Rad52*-Sepharose at the same salt concentration as Rad52* from ssDNA cellulose. The DNA binding was specific to Rad52* because no DNA was retained on a BSA-Sepharose column (unpublished results). Next, we investigated whether common cofactors such as Mg^{2+} or ATP would enhance binding of ssDNA. In fact, the presence of Mg^{2+}, ATP, or both together had a slightly adverse effect on binding (Fig. 3). The DNA binding of Rad52* has no absolute requirement for a free end because closed circular DNA eluted from the Rad52*-Sepharose at approximately the same NaCl concentrations as observed with linear dsDNA (unpublished results).

Rad52* Stimulates the Annealing of Complementary Oligonucleotides. Intermediates in homologous recombination are believed to involve branched molecules either as the result of a strand invasion event or later as a fully formed Holliday junction. We therefore tested an oligonucleotide-derived Y-structure (Fig. 4*A*), as well as a synthetic Holliday junction (31), for binding to Rad52*. The elution profiles of these substrates were similar to the one obtained with ssDNA (unpublished results). However, during our work with Y-structures, we found that oligo-C and oligo-D could not readily be annealed if mixed and incubated at 25°C (Fig. 4*B*). However, by adding Rad52* to oligo-C and oligo-D, a high yield of Y-structure could readily be formed at 25°C. The increase in annealing was not due to *E. coli* proteins present in the Rad52* preparation because a parallel purification from an extract obtained from a pQE60-Rad52*-His_6 derivative, which harbors a frameshift mutation created by deletion of the nucleotides encoding aa 49–261, failed to yield detectable Rad52*-derived protein, as well as any detectable annealing activity in any fractions eluted from the ssDNA column (unpublished results).

To investigate the annealing reaction, oligo-C and ^{32}P end-labeled oligo-D were incubated with various amounts of Rad52*. Fig. 4*B* shows that the substrates can be completely converted into the slower migrating Y-structure with increasing concentrations of Rad52*. Even at very low protein

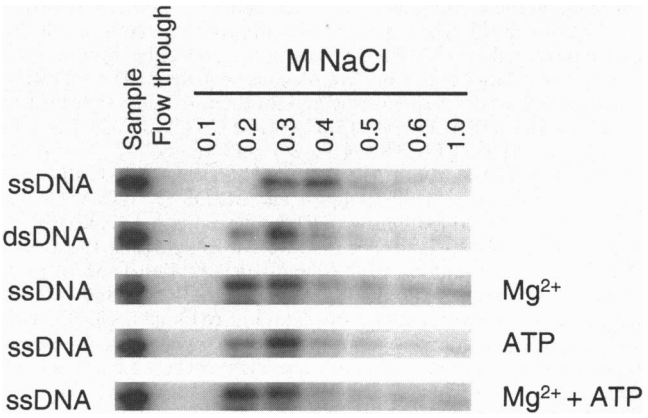

FIG. 3. ssDNA and dsDNA bind Rad52*-Sepharose. ssDNA and dsDNA were bound and eluted from Rad52*-Sepharose in the absence and presence of Mg^{2+} and ATP, as indicated.

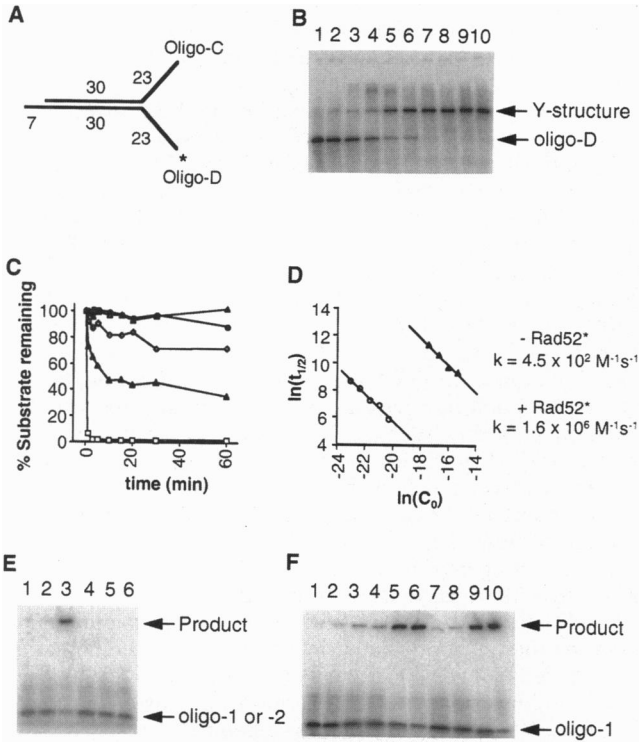

FIG. 4. Rad52* stimulates DNA strand annealing. (*A*) The Y-structure formed by annealing oligo-C (5′-**CGGAGCTTCCGGAGCTTCCTCTGGTGAGTG**GCGTCACTCTCCAAGGTGGCGGC-3′) and oligo-D (5′-CTTCGTTATCGTTTCGTCAGGAT**CACTCACCAGAGGAAGCTCCGGAAGCTCCGC**TTATCG-3′). The boldface nucleotides indicate the 30 bases in each oligonucleotide that can pair. (*B*) Annealing stimulated by Rad52*. Lane 1, oligo-D alone; lane 2, oligo-C and oligo-D; lanes 3–8, oligo-C, oligo-D, and Rad52* varying from 0.9 to 271 nM (0.9, 2.71, 9.03, 27.1, 90.3, and 271 nM, respectively); lane 9, the same amount of Rad52* as in lane 7 was preincubated for 1 hr before the addition of DNA; lane 10, as for lane 9 except that oligo-C was included in the preincubation with the protein and was followed by the addition of oligo-D. The final concentrations of oligo-C and ^{32}P end-labeled oligo-D were 4 nM and 2 nM, respectively. (*C*) Kinetics of Rad52*-stimulated annealing. Here we show the reaction conditions described in lanes 2 (●), 4 (◇), 5 (▲), and 7 (□) of *B*. A reaction including 500 nM BSA (△) was also studied. Annealing was measured as the disappearance of ssDNA oligo-D and plotted as a function of time. (*D*) Rad52*-stimulated strand annealing is a second-order reaction. The logarithm of the half-time, $t_{1/2}$, of the spontaneous (△), as well as the Rad52*-stimulated (○) annealing reaction in seconds plotted as a function of the logarithm of the initial molar concentration of nucleotides, C_0, are shown. Only nucleotides present in the homologous region were taken into consideration in the calculation of C_0. Each data set was fitted to $\ln(t_{1/2}) = -\ln(C_0) - \ln(k)$, where k is the second-order rate constant of the annealing reaction. (*E*) Rad52* promotes annealing even in the presence of a large excess of heterologous sequences. The following two oligonucleotides were investigated for their to ability to hybridize to M13mp18 ssDNA: Oligo-1 (5′-CATGGTCATAGCTGTTTCCTGTGTGAAATTGTTATCCGCTC-3′) and oligo-2 (5′-GAGCGGATAACAATTTCACACAGGAAACAGCTATGACCATG-3′) Lane 1, oligo-1 alone; lane 2, oligo-1 and M13mp18 ssDNA; lane 3, oligo-1, Rad52*, and M13mp18 ssDNA; lane 4, oligo-2 alone; lane 5, oligo-2 and M13mp18; lane 6, oligo-2, Rad52*, and M13mp18 ssDNA. The final concentrations of ^{32}P end-labeled oligo-1 or oligo-2, M13mp18 ssDNA and Rad52* were 0.2 nM, 0.4 nM, and 90 nM, respectively. (*F*) Preincubation of oligo-1 or M13mp18 ssDNA with Rad52* prior to the addition of M13mp18 ssDNA or oligo-1, respectively, does not alter the yield of the annealing reaction. Lane 1, oligo-1 alone; lane 2, oligo-1 and M13mp18 ssDNA; lanes 3–6, oligo-1 preincubated for 5 min on ice in the presence of 3, 10, 30, and 90 nM Rad52*, respectively, before addition of M13mp18 ssDNA; lanes 7–10, M13mp18 ssDNA preincubated for 5 min on ice in the presence of 3, 10, 30, and 90 nM Rad52*, respectively, before addition of oligo-1. The final concentration of ^{32}P end-labeled oligo-2 and M13mp18 ssDNA was as in *E*.

concentrations (a molar ratio of Rad52* to total oligonucleotide molecules of 0.5, lane 4), we found significantly more product formation than in the spontaneous reaction (lane 2). At a molar excess of Rad52* to total oligonucleotide molecules of 1.5, more than one-half of the substrate was converted into product (lane 5). At these low Rad52* concentrations, we noticed a stable, slower migrating species, in addition to the Y-structure (lanes 4 and 5). Whether this species represents a side reaction or a potential intermediate remains to be established. The activity of Rad52* was stable during the reaction time because the protein could be preincubated for 1 hour at reaction conditions in either the absence of DNA (lane 9) or the presence of one of the oligonucleotides (lane 10) without losing subsequent annealing ability.

Annealing Is a Second-Order Reaction. The kinetics of several reactions shown in Fig. 4*B* were also studied (Fig. 4*C*). As expected, the spontaneous reaction and a control reaction containing an 80-fold molar excess of BSA to total oligonucleotide molecules were both slow. In contrast with a 15-fold molar excess of Rad52*, the annealing reaction was rapid and most of the substrate was converted into product in 1 min. At lower concentrations of Rad52*, the substrate was only partially converted into annealed structures. These reactions progressed in a biphasic manner. First, in the rapid phase, the amount of substrate consumed depended on the amount of Rad52* in the reaction. In the slower second phase, the remaining oligonucleotides annealed at a rate that resembles that of the spontaneous reaction. This is most likely explained by Rad52* being present in limiting concentrations for annealing and, furthermore, that it remains bound to the product. Unbound DNA anneals at the rate of the spontaneous reaction accounting for the second phase. The stoichiometry of the reactions suggests that only a few Rad52* molecules (perhaps only one) per oligonucleotide, are required for an annealing event to take place.

The mechanisms of the Rad52*-stimulated annealing reaction at saturating protein concentration and the spontaneous reaction were investigated by measuring the half-time of Y-structure formation at different initial DNA concentrations. A log–log plot of the half-times of the annealing reactions versus the initial DNA concentrations yielded straight lines with slopes of −1.0 and −0.98 for the spontaneous and the Rad52*-stimulated reaction, respectively. The fact that these slopes do not differ from −1 indicates that both reactions follow second-order kinetics (Fig. 4*D*). This suggests that the rate-limiting step is determined by the frequency of the encounters by individual DNA–Rad52* complexes (or simply oligo-C with oligo-D in the spontaneous reaction) and not by a subsequent annealing step, which would result in first-order kinetics. A comparison of the two rate constants showed that the annealing reaction is 3500-fold faster when Rad52* is included. The fact that Rad52* stimulates annealing without any additional energy requirement (e.g., ATP) is in accordance with DNA annealing being a thermodynamically favorable reaction that proceeds spontaneously at 25°C, albeit at a slow rate.

Rad52*-Stimulated Annealing Is Homology Dependent. The annealing reaction presented above could be the result of Rad52* bringing two complementary oligonucleotides close together in a manner that is DNA-homology independent. If this were the ease, the annealing reaction would be considered an accidental by-product of the DNA binding ability of Rad52*. To rule out this possibility, we investigated whether Rad52* is capable of stimulating the annealing of an oligonucleotide to a target sequence in a complex background. Two complementary 41-mer oligonucleotides were synthesized. Oligo-1 anneals to M13mp18 ssDNA, whereas oligo-2 does not. Fig. 4*E* shows that in the presence of Rad52* and M13mp18, oligo-1 is present in a high molecular weight product (lane 3). In contrast, the spontaneous reaction is very slow and the high molecular weight product is barely

detectable (lane 2). As expected, oligo-2 did not anneal to M13mp18 even in the presence of Rad52* (lanes 5 and 6). A control experiment showed that the annealing ability of oligo-2 was unimpaired since it was capable of hybridizing to oligo-1 (unpublished results). The yield of the annealing reaction did not depend on whether Rad52* was preincubated with either one of the substrates prior to the addition of the second one (Fig. 4*F*). Thus, the 180-fold excess of nonhomologous DNA present in the M13mp18 backbone in the preincubation step does not inhibit the subsequent annealing reaction.

DISCUSSION

We have shown that Rad52* is capable of annealing two complementary oligonucleotides at a rate that is 3500-fold stimulated compared with the spontaneous rate of annealing, and that the reaction obeys second-order kinetics (Fig. 4*D*). Importantly, this annealing activity is dependent upon DNA homology (Fig. 4*E*). The physiological importance of this annealing reaction awaits the characterization of a *rad52* mutant that is incapable of performing this activity *in vitro*. However, several lines of evidence suggest that the strand annealing property of Rad52* is biologically relevant. The inferred single-strand annealing component of direct repeat recombination is dependent on *RAD52* (32). *RAD52* function is required for inverted repeat recombination whether the substrates are present on plasmids (33) or in the chromosome (34). Furthermore, chromosomal inverted repeat recombination is almost completely independent of the three mitotically expressed RecA homologs Rad51, Rad55, and Rad57 (35). Similarly, we have found that formation of Holliday junction intermediates in the rDNA multiple-tandem array requires *RAD52* but not *RAD51*, *RAD55*, and *RAD57* (H. Zou and R.R., unpublished results). These observations emphasize the importance of Rad52 function for some recombination events even when the yeast RecA homologs are not required.

The dramatic increase in the reannealing rate of a small DNA fragment in the presence of Rad52* is virtually identical to that obtained with A1 heterogeneous nuclear ribonucleoprotein in a comparable reaction, but not with the small increase observed using *E. coli* ssDNA binding protein (36). This suggests that Rad52* acts mostly by elevating the effective concentration of DNA and less by dissolving intramolecular secondary DNA structures or by reducing electrostatic repulsion of the negatively charged oligonucleotides (36). Pontius and Berg (36) argued that such an elevation may be obtained if a protein mediates an increased number of rapid transient encounters between individual protein–DNA molecules. The presence of a self-association domain in Rad52 (26) could account for such a mechanism.

As the role of A1 heterogeneous nuclear ribonucleoprotein protein *in vivo* is thought to facilitate rapid association of homologous RNA (36), it is tempting to imagine a similar role for Rad52*, but at the level of DNA. Since an early intermediate during homologous recombination is a double-strand break (37), it is easy to envision that both a successful recombination event and survival itself would require a mechanism to localize a homologous intact partner quickly to initiate the subsequent repair event. Physical studies during mating type interconversion in the absence of the *RAD52* gene show that double-strand break intermediates persist *in vivo* and that strand invasion is abolished (38). The biochemical characterization of Rad52 described here suggests that this is due to an inability to anneal and start the reaction. Most recombination reactions, including mating type switching, also require other genes from the *RAD52* epistasis group suggesting the requirement of a more complex machinery. Indeed, several of these genes interact physically (39, 40), specifically Rad51 and Rad52 (26, 27). Thus, recombination in a Rad52-initiated reaction may proceed by the ability of Rad51 to form filaments on DNA and catalyze strand exchange (7–9).

We thank A. Eggleston, N. Erdeniz, S. Gangloff, J. Smith, S. Sturley, L. Symington, and H. Zou for comments on the manuscript. We also thank A. Shinohara and T. Ogawa for sharing unpublished data, B. Stillman for helpful suggestions, and L. Ruwitch and M. Lee for excellent technical assistance. The work was supported by the Danish Cancer Society (C.B.), the Carlsberg Foundation (U.H.M.), the Danish Natural Science Research Council (U.H.M.), and the National Institutes of Health (R.R.).

1. Emery, H. S., Schild, D., Kellogg, D. E. & Mortimer, R. K. (1991) *Gene* **104,** 103–106.
2. Carlson, M. & Laurent, B. C. (1994) *Curr. Opin. Cell Biol.* **6,** 396–402.
3. Bishop, D. K., Park, D., Xu, L. & Kleckner, N. (1992) *Cell* **69,** 439–456.
4. Shinohara, A., Ogawa, H. & Ogawa, T. (1992) *Cell* **69,** 457–470.
5. Lovett, S. T. (1994) *Gene* **142,** 103–106.
6. Kans, J. A. & Mortimer, R. K. (1991) *Gene* **105,** 139–140.
7. Ogawa, T., Yu, X., Shinohara, A. & Egelman, E. H. (1993) *Science* **259,** 1896–1899.
8. Sung, P. (1994) *Science* **265,** 1241–1243.
9. Sung, P. & Robberson, D. L. (1995) *Cell* **82,** 453–461.
10. Resnick, M. A. (1969) *Genetics* **62,** 519–531.
11. Petes, T. D., Malone, R. E. & Symington, L. S. (1991) in *The Molecular and Cellular Biology of the Yeast Saccharomyces: Genome Dynamics, Protein Synthesis and Energetics*, eds. Broach, J. R., Pringle, J. R. & Jones, E. W. (Cold Spring Harbor Lab. Press, Plainview, NY), Vol. 1, pp. 407–521.
12. Game, J. C. (1993) *Semin. Cancer Biol.* **4,** 73–83.
13. Friedberg, E. C. (1991) *BioEssays* **13,** 295–302.
14. Game, J. C., Zamb, T. J., Braun, R. J., Resnick, M. & Roth, R. M. (1980) *Genetics* **94,** 51–68.
15. Prakash, S., Prakash, L., Burke, W. & Monteleone, B. (1980) *Genetics* **94,** 31–50.
16. Resnick, M. A., Nitiss, J., Edwards, C. & Malone, R. E. (1986) *Genetics* **113,** 531–550.
17. Hoekstra, M. F., Naughton, T. & Malone, R. E. (1986) *Genet. Res.* **48,** 9–17.
18. Malone, R. E. & Esposito, R. E. (1980) *Proc. Natl. Acad. Sci. USA* **77,** 503–507.
19. Ostermann, K., Lorentz, A. & Schmidt, H. (1993) *Nucleic Acids Res.* **21,** 5940–5944.
20. Bezzubova, O. Y., Schmidt, H., Ostermann, K., Heyer, W. D. & Buerstedde, J. M. (1993) *Nucleic Acids Res.* **21,** 5945–5949.
21. Muris, D. F., Bezzubova, O., Buerstedde, J. M., Vreeken, K., Balajee, A. S., Osgood, C. J., Troelstra, C., Hoeijmakers, J. H., Ostermann, K., Schmidt, H., Natarajan, A. T., Eeken, J. C. J., Lohman, P. H. M. & Pastink, A. (1994) *Mutat. Res.* **315,** 295–305.
22. Bendixen, C., Sunjevaric, I., Bauchwitz, R. & Rothstein, R. (1994) *Genomics* **23,** 300–303.
23. Adzuma, K., Ogawa, T. & Ogawa, H. (1984) *Mol. Cell. Biol.* **4,** 2735–2744.
24. Schild, D., Calderon, I. L., Contopoulou, R. & Mortimer, R. K. (1983) in *Cellular Responses to DNA Damage*, eds. Bridges, B. A. & Friedberg, E. C. (Liss, New York), pp. 417–427.
25. Ogawa, T., Shinohara, A., Nabetani, A., Ikeya, T., Yu, X., Egelman, E. H. & Ogawa, H. (1993) *Cold Spring Harbor Symp. Quant. Biol.* **58,** 567–576.
26. Milne, G. T. & Weaver, D. T. (1993) *Genes Dev.* **7,** 1755–1765.
27. Shinohara, A., Ogawa, H. & Ogawa, T. (1992) *Cell* **69,** 457–470.
28. Firmenich, A. A., Elias-Arnanz, M. & Berg, P. (1995) *Mol. Cell. Biol.* **15,** 1620–1631.
29. Thomas, B. J. & Rothstein, R. (1989) *Cell* **56,** 619–630.
30. Harashima, S., Shimada, Y., Nakade, S. & Oshima, Y. (1989) *Curr. Genet.* **219,** 495–498.
31. Connolly, B., Parsons, C. A., Benson, F. E., Dunderdale, H. J., Sharples, G. J., Lloyd, R. G. & West, S. C. (1991) *Proc. Natl. Acad. Sci. USA* **88,** 6063–6067.
32. Ozenberger, B. A. & Roeder, G. S. (1991) *Mol. Cell. Biol.* **11,** 1222–1231.
33. Dornfeld, K. J. & Livingston, D. M. (1992) *Genetics* **131,** 261–276.
34. Rattray, A. J. & Symington, L. S. (1994) *Genetics* **138,** 587–95.

35. Rattray, A. J. & Symington, L. S. (1995) *Genetics* **139,** 45–56.
36. Pontius, B. W. & Berg, P. (1990) *Proc. Natl. Acad. Sci. USA* **87,** 8403–8407.
37. Sun, H., Treco, D., Schultes, N. P. & Szostak, J. W. (1989) *Nature (London)* **338,** 87–90.
38. White, C. I. & Haber, J. E. (1990) *EMBO J.* **9,** 663–673.
39. Hays, S. L., Firmenich, A. A. & Berg, P. (1995) *Proc. Natl. Acad. Sci. USA* **92,** 6925–6929.
40. Johnson, R. D. & Symington, L. S. (1995) *Mol. Cell. Biol.* **15,** 4843–4850.